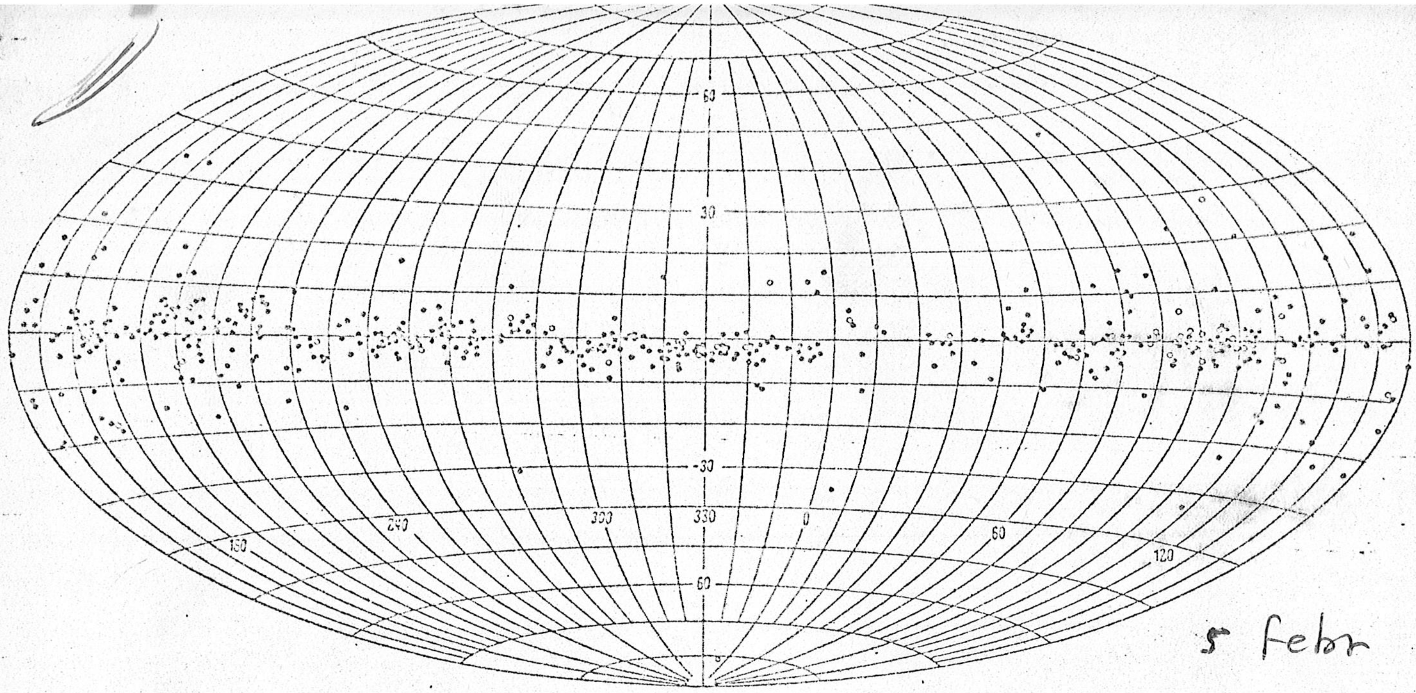

← fig 1

5 febr

Fig. 2. Distributin of galactic clusters in galactic coordinates. Open circles are clusters added since COLLINDER's Catalogue.

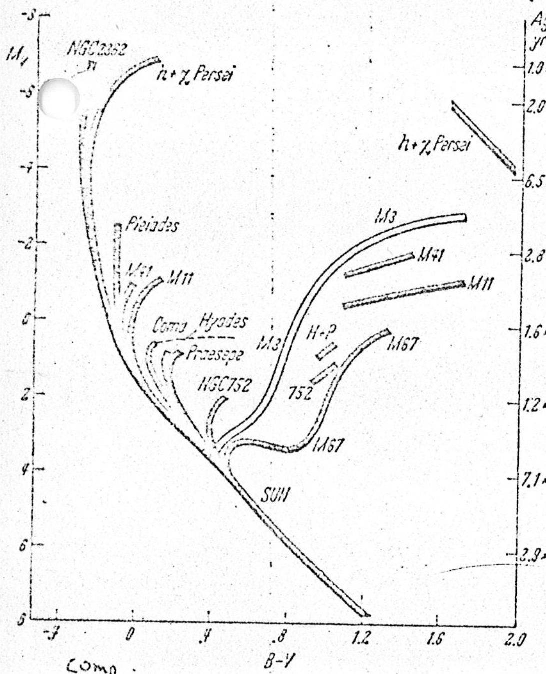

Comp.

Fig. [illegible] Composite color-magnitude diagram by SANDAGE for 11 clusters. Astrophys. Journ. 125, 435 (1957).

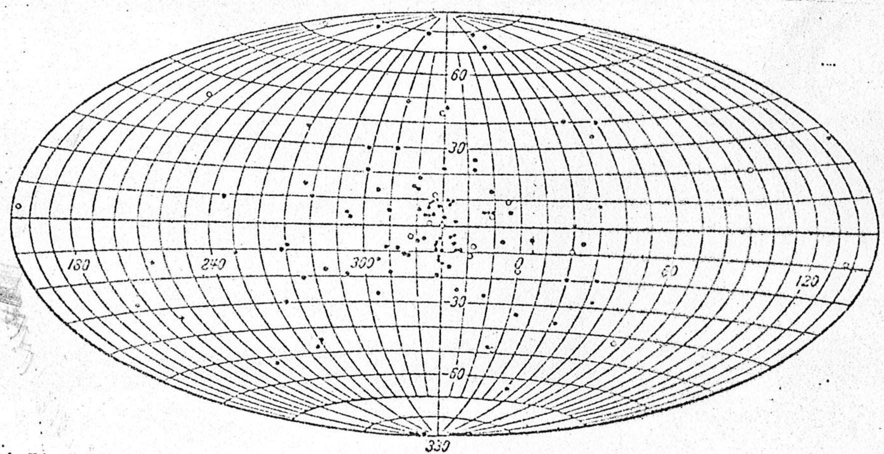

Fig. 16. Distribution of globular clusters in galactic co-ordinates. Open circles are clusters added to globular list since 19

← fig 2   fig 4 ↑   fig 5 ↓

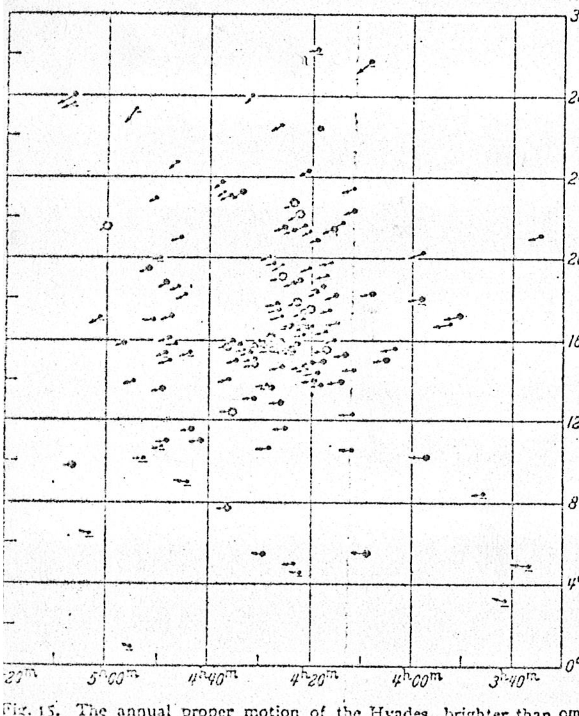

Fig. 15. The annual proper motion of the Hyades, brighter than 9m0 visual, by VAN BUEREN. Bull. Astronom. Inst. Netherl. 11, 385 (1952).

← fig 13

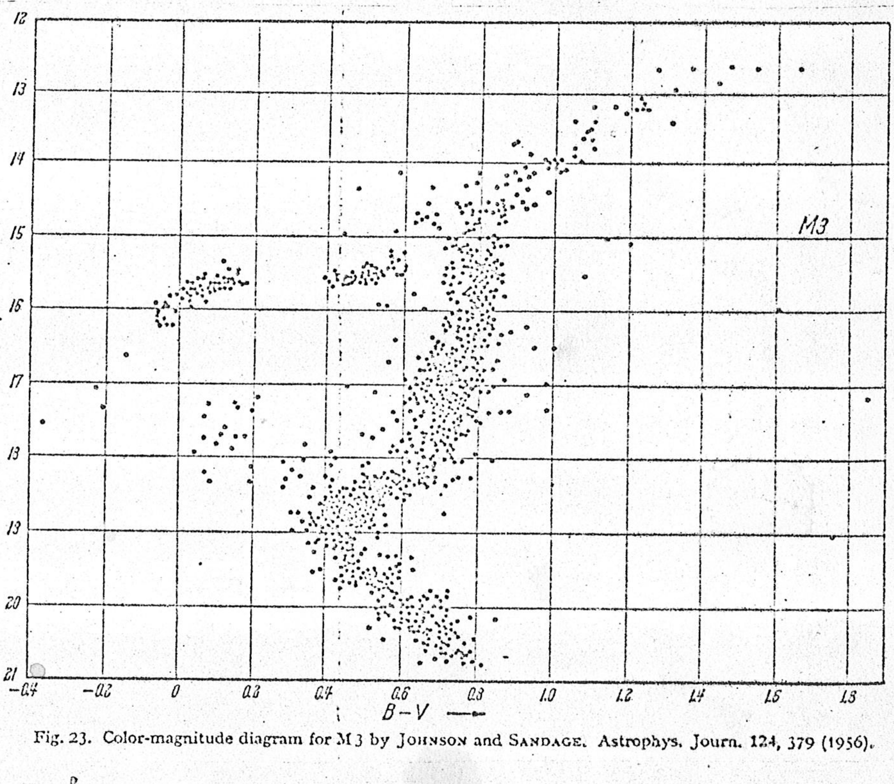

Fig. 23. Color-magnitude diagram for M3 by JOHNSON and SANDAGE. Astrophys. Journ. 124, 379 (1956).

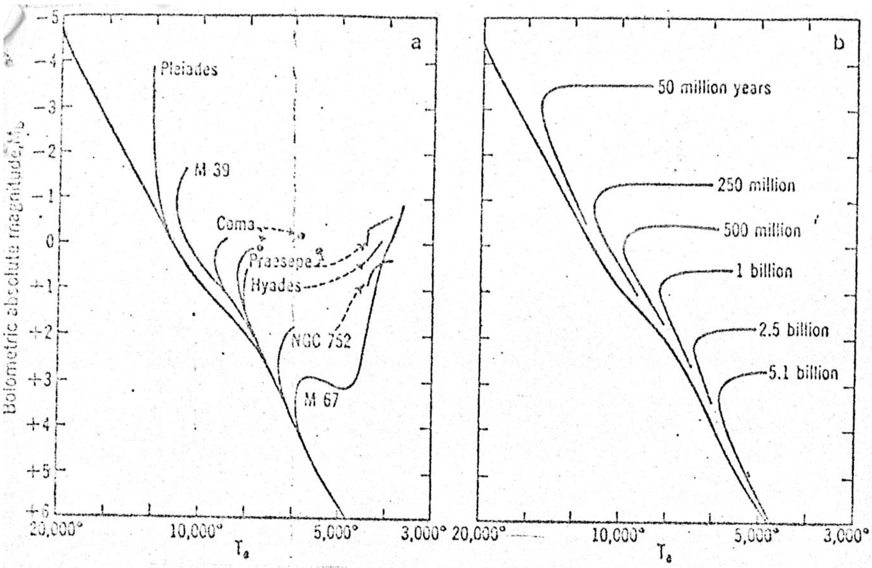

← fig.6

vanuit de waarn. gezien
z-as naar de waarn.

van "boven" gezien
ρ = afstand tot centrum
r = idem in projektie
R = straal bolhoop

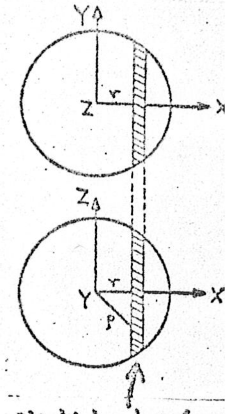

fig 7

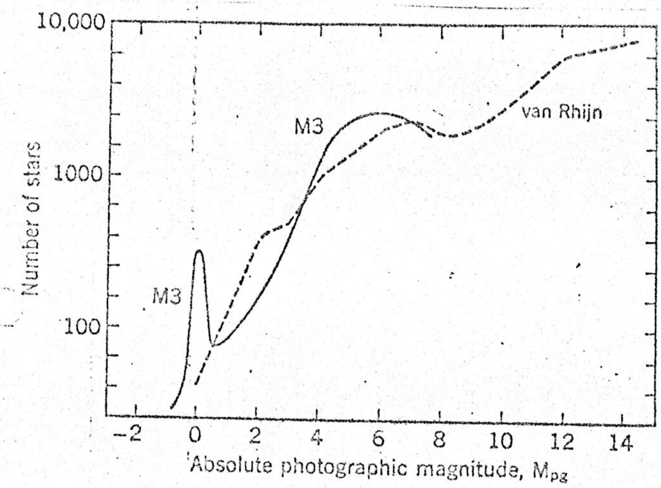

Fig. 55. The luminosity function for Messier 3. Sandage has counted stars in successive intervals of photographic absolute magnitude in the globular cluster Messier 3. In the diagram his derived luminosity function is compared with that of van Rhijn in Fig. 40, which applies to the vicinity of the sun. (Courtesy of *Astronomical Journal.*)

← fig 11

Leuchtkraftfunktion

N = Zahl/1000 pc^3 (Bereich $M \pm 1/2$)

$\varphi(M)$ = beobachtete LKF (Hauptreihe)

$\psi(M)$ = ursprüngliche LKF = LKF_0

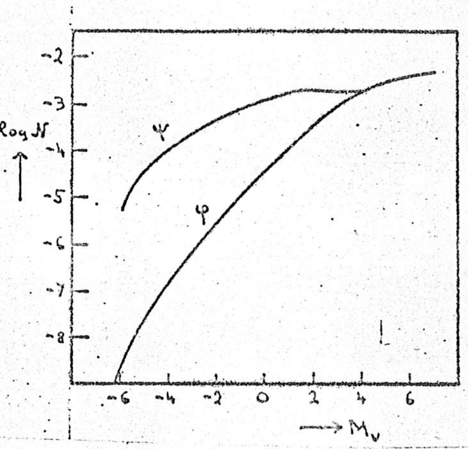

fig 13 ↑

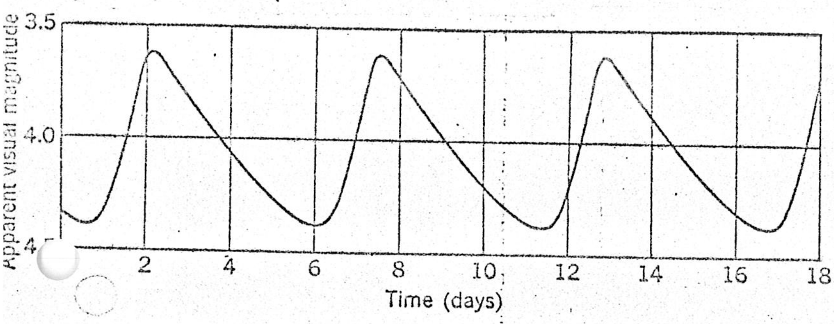

Fig. 50. Light curve of Delta Cephei. The diagram illustrates the changes in apparent magnitude. The period of the light variation is 5 days 9 hours.

fig 9.

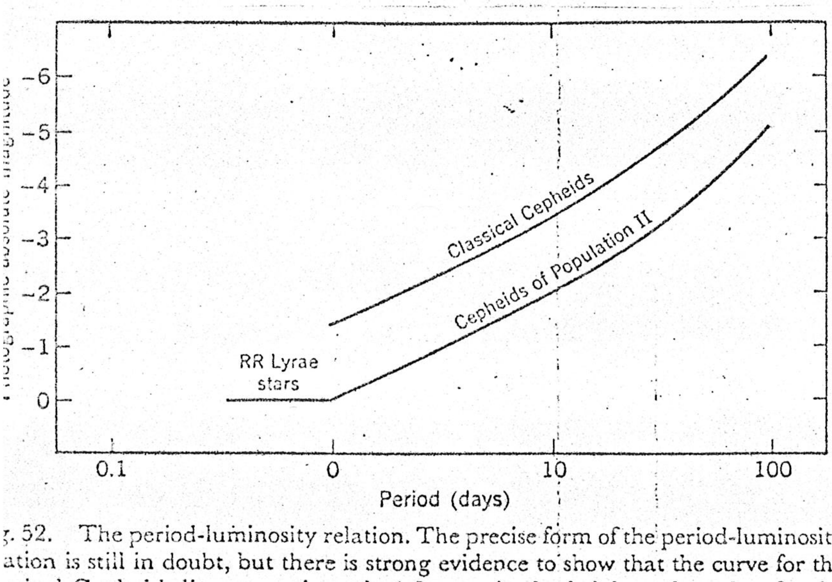

Fig. 52. The period-luminosity relation. The precise form of the period-luminosity relation is still in doubt, but there is strong evidence to show that the curve for the classical Cepheids lies approximately 1.5 magnitudes brighter than that for the Population II Cepheids.

← fig 10

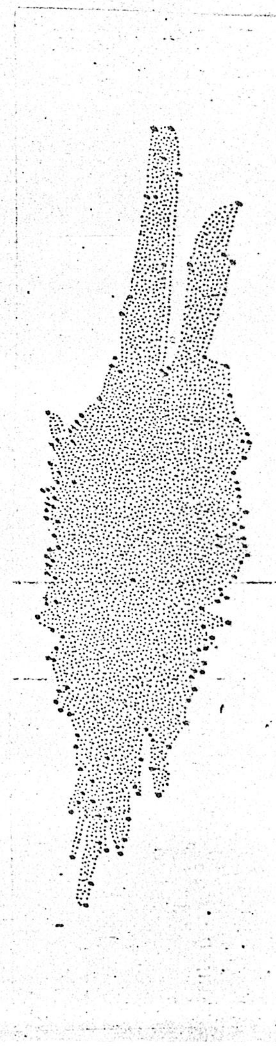

Fig. 1. Section of the galactic system according to Sir William Herschel's first theory (1785).

fig 8

V (3)

Fig. 12

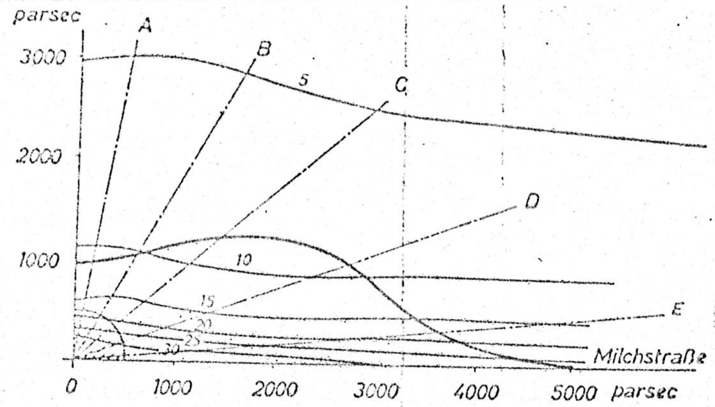

Fig. 3b. The stellar system according to Seeliger (1922).

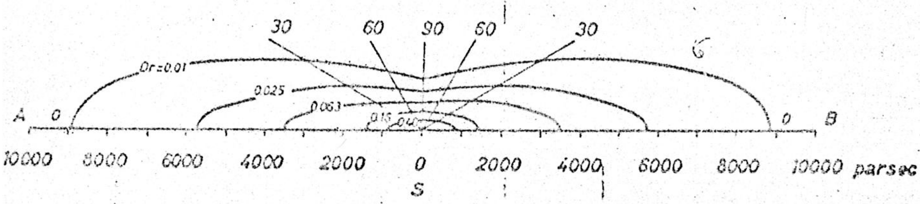

Fig. 4. The stellar system according to Kapteyn-van Rhijn (1920).

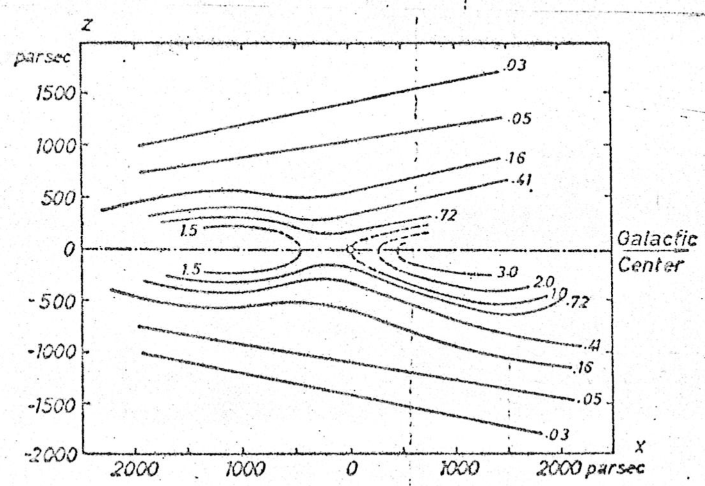

Fig. 10. General density distribution of all types of stars together according to Oort (1938), in the intersection of the galactic system with a plane perpendicular to that of the Galaxy, passing through the Sun and the centre of the system. The dotted parts of the equidensity lines are extrapolated. Unit of density is the density near the Sun.

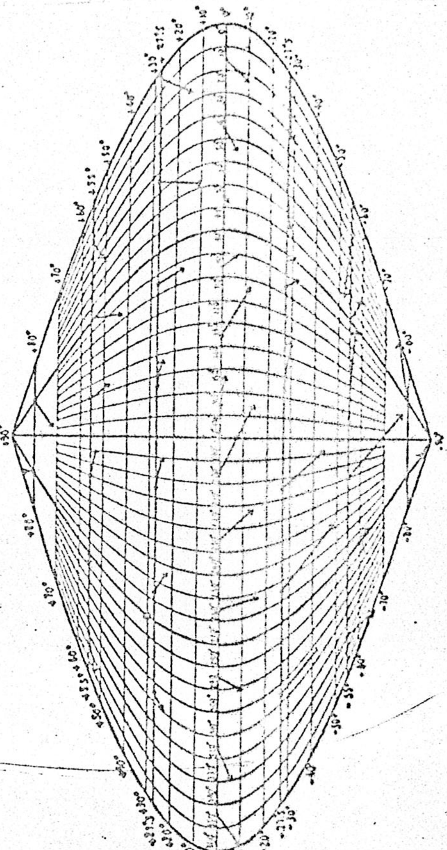

Fig. 39. The sun's motion from proper motions. The arrows represent the average directions and amount of proper motions for 726 A stars of the fifth apparent

fig 17 ↑

← Fig 14

fig 16 ↓

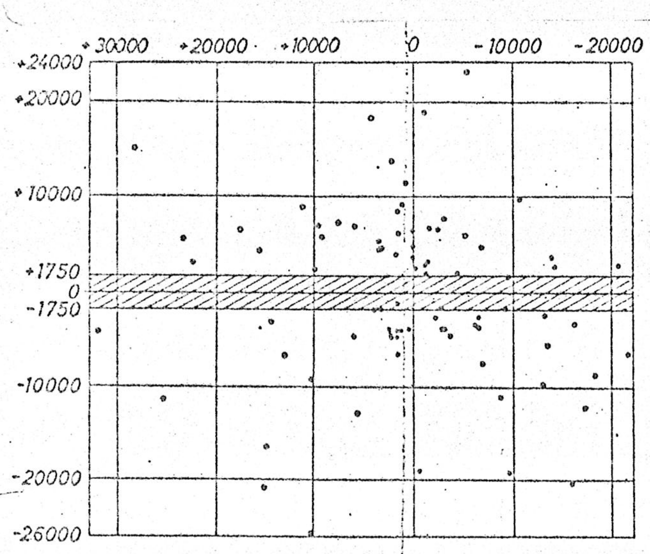

The globular clusters and the Milky Way, according to H. Shapley (1918).

fig 15 ↑

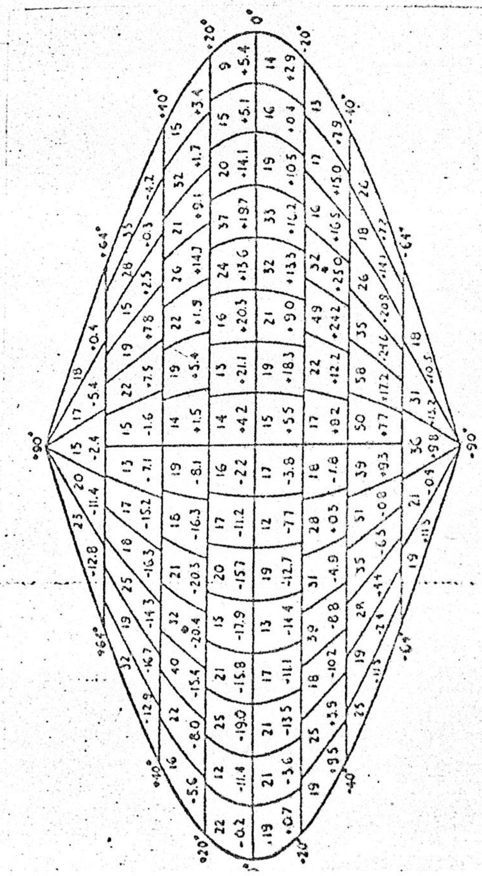

Fig. 38. The sun's motion from radial velocities. Averages of the radial velocities for 2149 naked-eye stars measured at the Lick Observatory. The position of the apex of the sun's motion is shown by a small circle near the position of greatest average negative radial velocity.

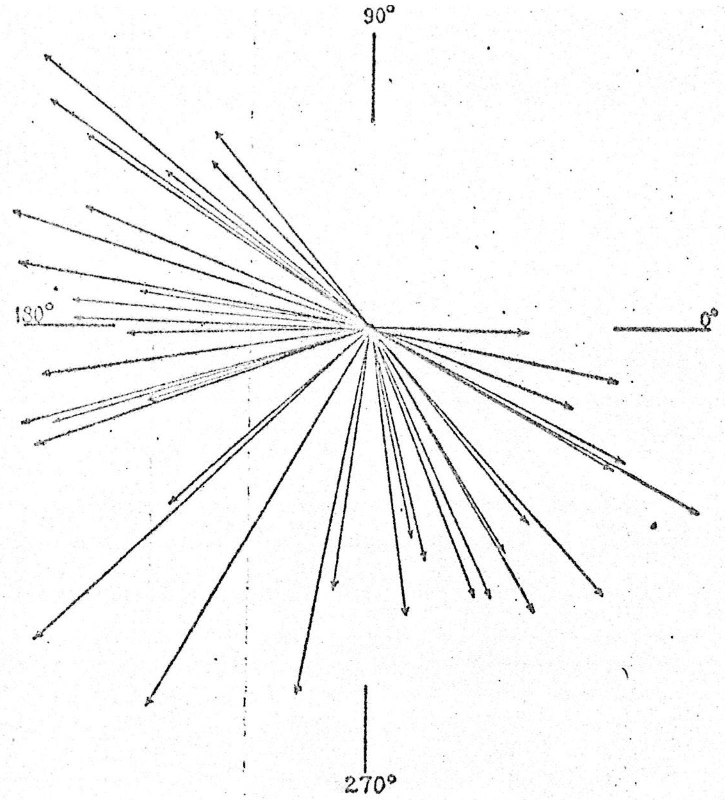

[Fi]g. 58. The asymmetry in stellar motions. The diagram gives the distribution in [the] ga[lact]ic plane of the directions of the velocities of nearby stars with speeds in [ex]cess of 60 km/sec. The galactic longitudes of these directions are indicated. Not [a s]ingle star in the diagram is found to move in a direction between galactic longi[tud]es $l = 350°$ and $l = 120°$; the center of the sector of avoidance is at $l = 55°$.

← 18

19 ↓ RG = v_r

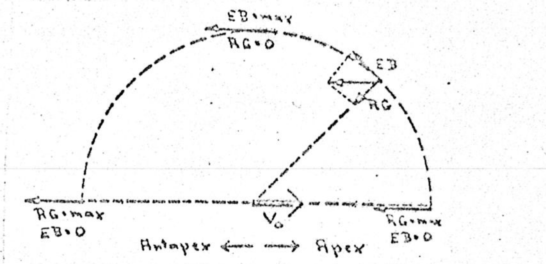

20 a ↓

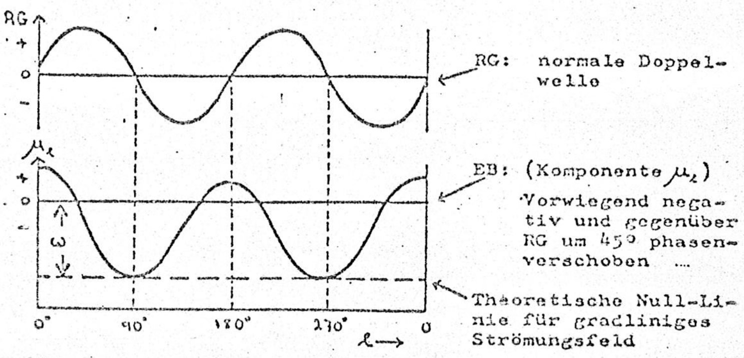

20 b ↑

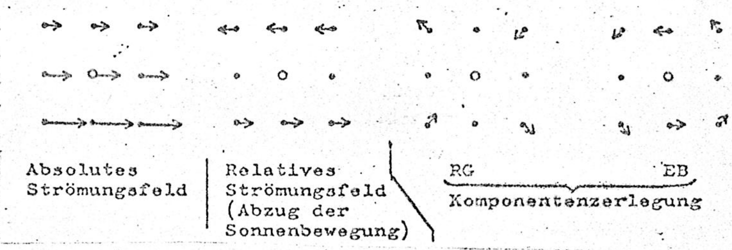

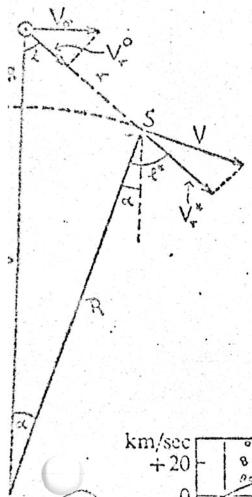

V_0 = Geschwindigkeit
R_0 = Abstand vom gal. Zentrum
ω_0 = Winkelgeschw.
} der Sonne

R, V(R), ω(R) } Dasselbe allgemein, am Ort des gerade betrachteten Sterns

l = gal. Länge
V_r^0 = Radialkomponente
} bezüglich Sonne → Stern

l^*; V_r^* Analoge Größen am Ort des Sterns

r = Abstand Sonne–Stern

21 ↑ 22 ↓

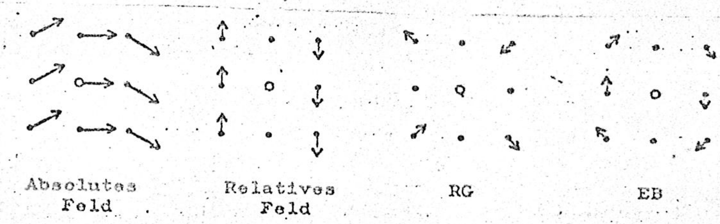

23 ↑

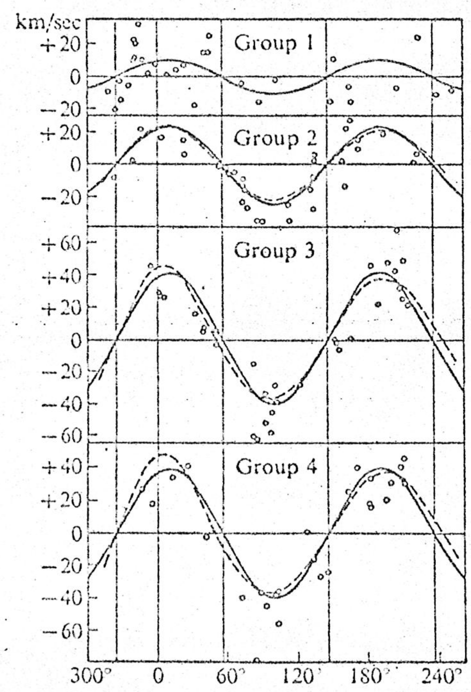

20 c ←

Fig. 8-11. Radial velocities of Cepheids observed by Joy. The solid curves are the radial velocities predicted by equation (8-12), with A = 25, 23, 24.5, and 17.1 (km/sec)/kpc for groups 1, 2, 3, and 4, respectively, yielding a mean value of A = 21 (km/sec)/kpc. Note that the abscissa is expressed in terms of the old longitude scale l^I. (From A. H. Joy,

24 →

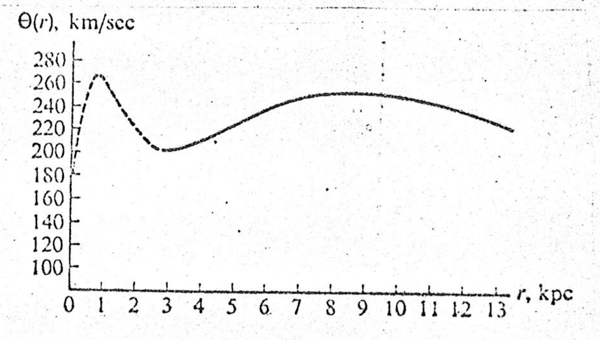

Fig. 8-18. The rotation curve Θ(r)

Kurven konstanter relativer Dichte im Milchstraßensystem (Modell M. Schmidt)

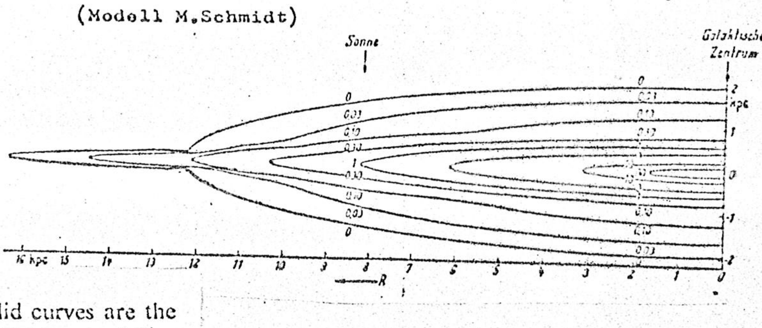

25 ↑

V (5)

26 ↓

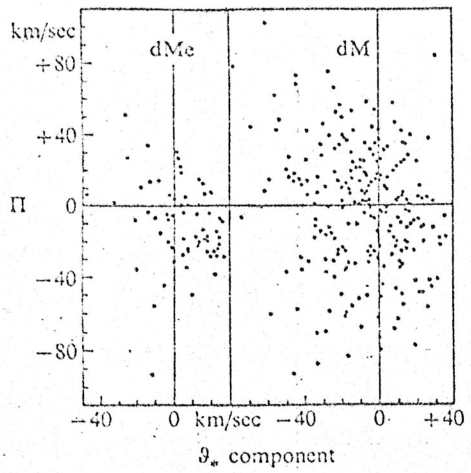

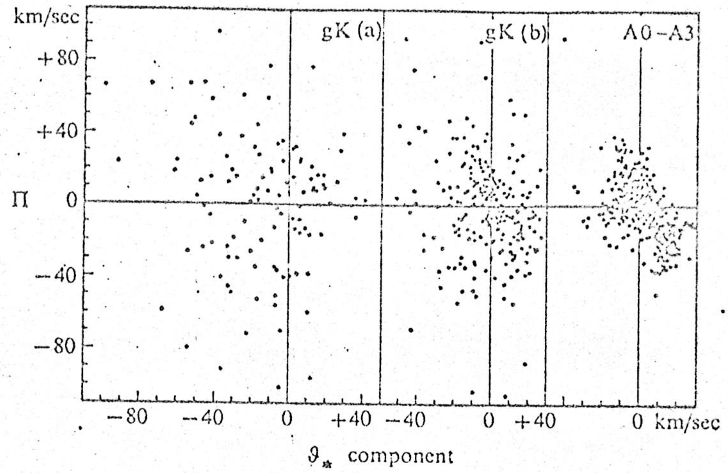

27 ←

FIG. 7-2. Kinematical differences between gK stars with (*a*) high Z velocities and (*b*) low Z velocities. Also shown are the velocities for main sequence A0-A3 stars. [From J. Delhaye, in A. Blaauw and M. Schmidt (eds.), *Galactic Structure*, Chicago: University of Chicago Press, 1965, chap. 4, by permission.]

FIG. 7-1. The distribution of Π and ϑ_* velocities for dM and dMe stars, showing the kinematical differences between these two stellar groups. [From J. Delhaye, in A. Blaauw and M. Schmidt (eds.), *Galactic Structure*, Chicago: University of Chicago Press, 1965, chap. 4, by permission.]

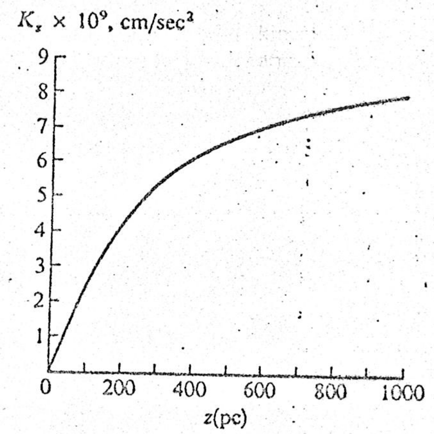

30 ←

FIG. 12-5. Quantitative run of K_z (in units of 10^{-9} cm/se

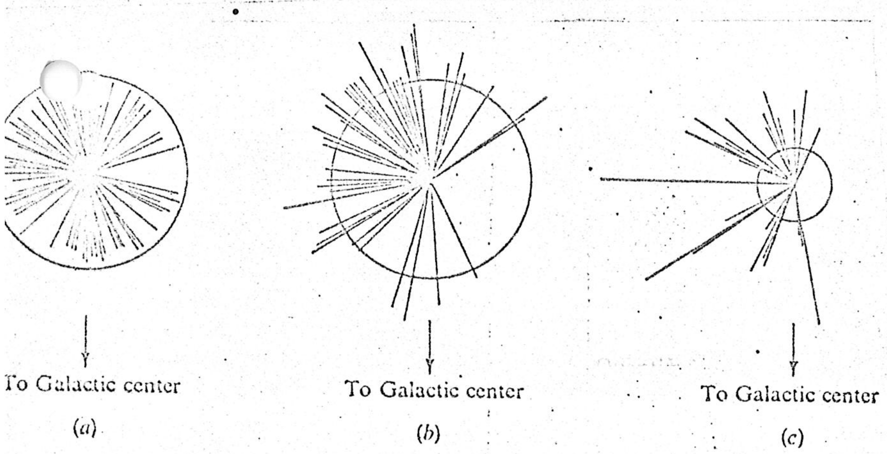

FIG. 7-4. The velocity vectors, relative to the LSR, of stars with (*a*) $v < 63$ km/sec,) $63 \leq v \leq 100$ km/sec, and (*c*) $v > 100$ km/sec. The circle has a radius of 63 km/sec each case. (After J. H. Oort, *Kapteyn Astron. Lab. Groningen Publ. 40*, 1926.)

29 ↑

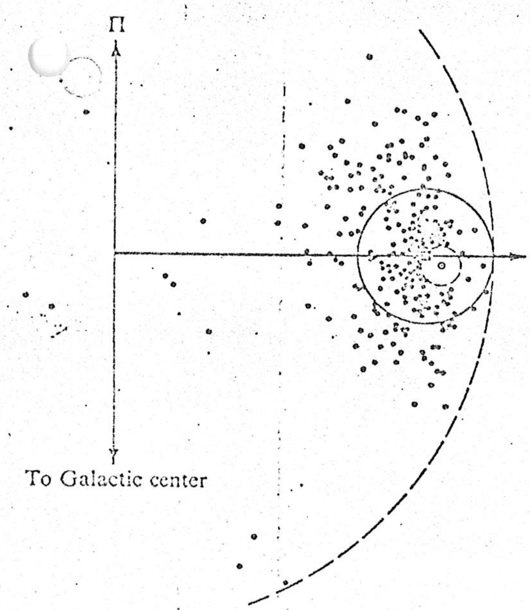

28 ←

32 →

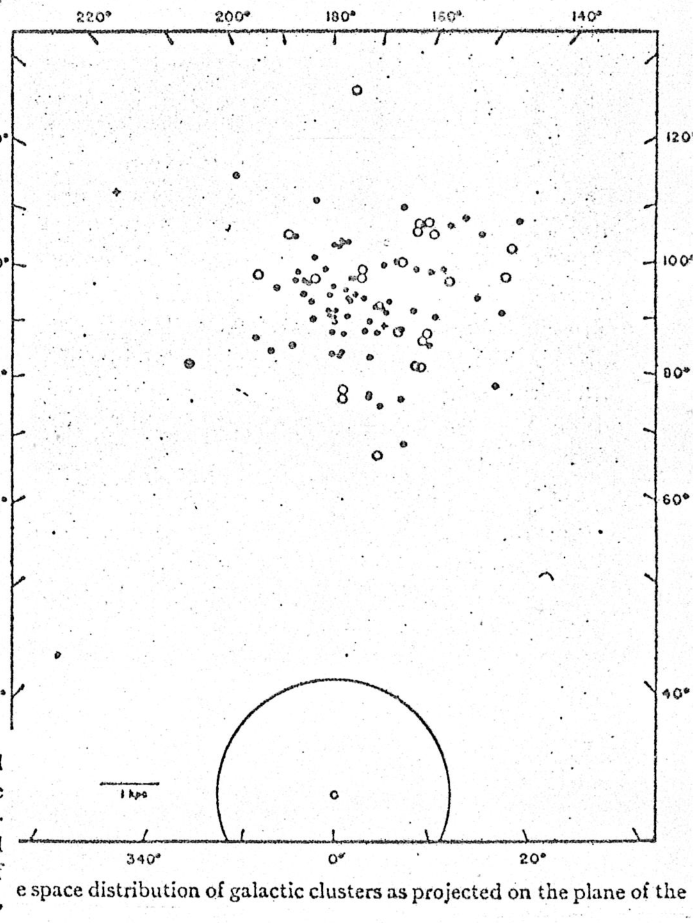

FIG. 7-3. The distribution of the Π and Θ velocities for high-velocity stars as derived y Oort in 1928. The square represents the LSR; the circled dot represents the sun. The nall dashed circle has a radius of 20 km/sec and excludes stars for which the observaonal sample is incomplete. The solid circle has a radius of 65 km/sec. No star is observed have a velocity greater than 65 km/sec with respect to the LSR in the direction of alactic rotation. No stars are observed to have velocities outside the large dashed circle, hich has a radius of 365 km/sec. (After J. H. Oort, *Bull. Astron. Inst. Netherlands*, 4, 269,

e space distribution of galactic clusters as projected on the plane of the

V. 6

33

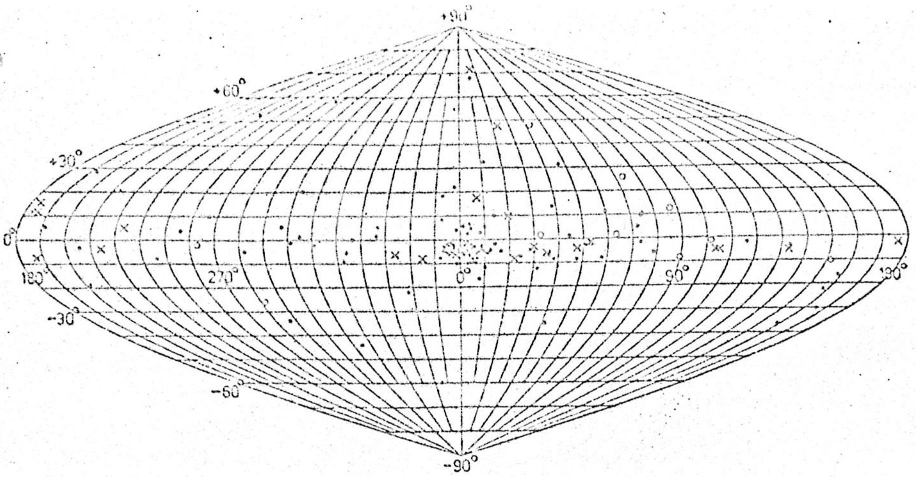

FIG. 1.—The distribution of novae in the sky. New galactic coordinates l^{II}, b^{II} are used. Circles: $m_{max} < 3.0$; crosses: $3.0 \leq m_{max} < 6.0$; dots: $6.0 \leq m_{max}$.

31

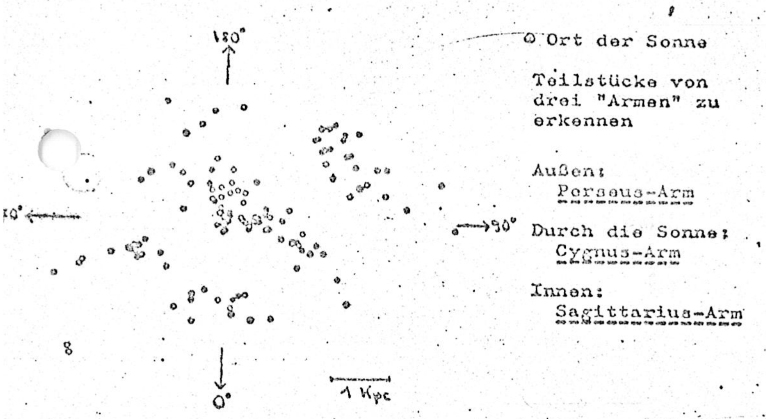

34

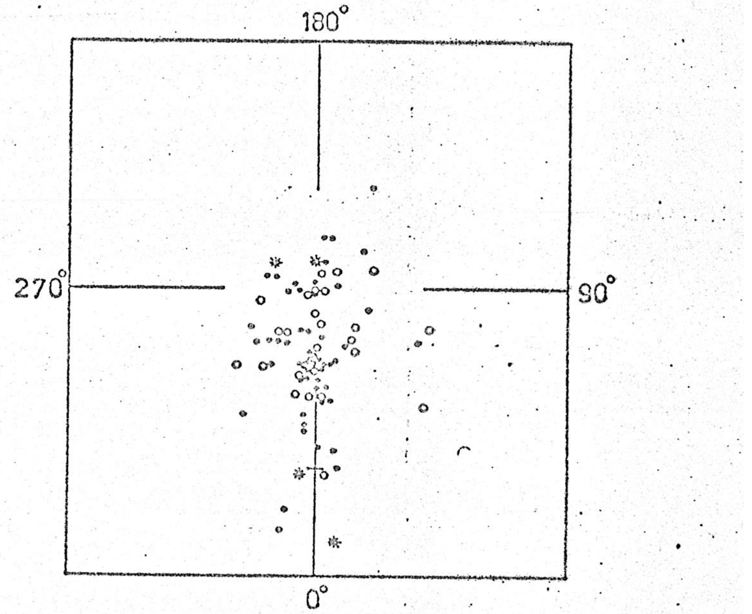

FIG. 3.—Projection of positions of novae on the galactic plane. Dots, circles, and stars denote fast, slow, and very slow novae, respectively. New galactic longitudes are shown at the margin. The short horizontal line at $l = 0°$ denotes the position of the galactic center. (From Payne-Gaposchkin 1957, Fig. 2.3.)

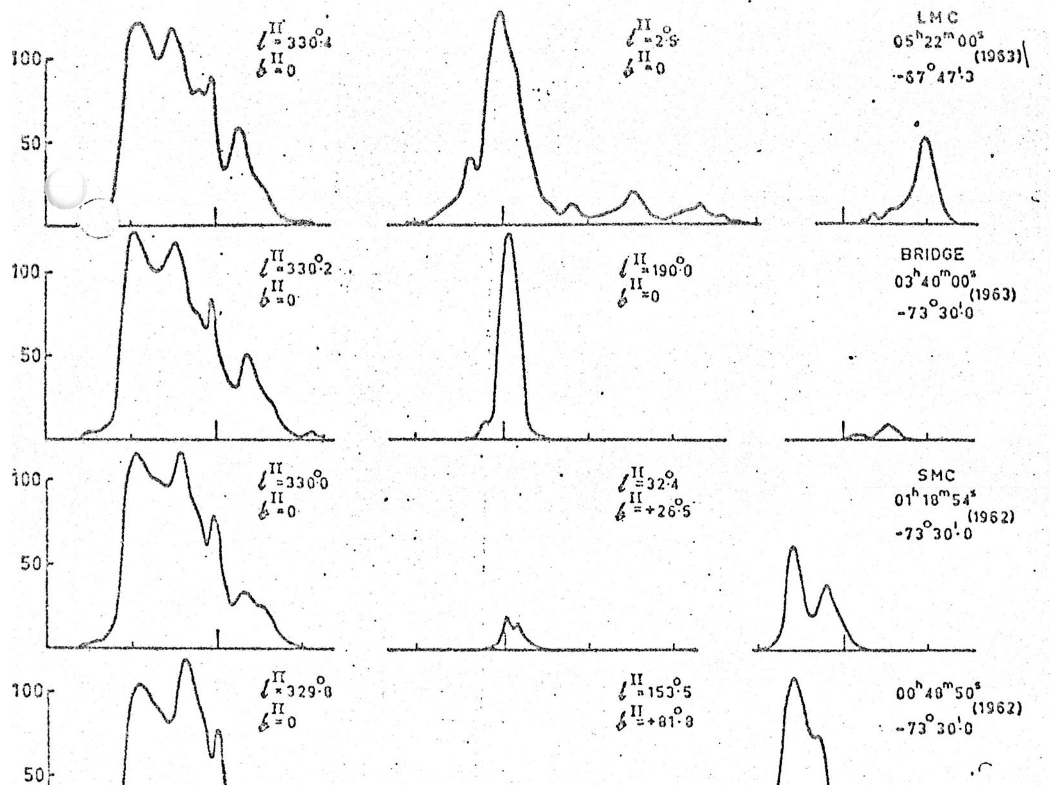

FIG. 4.—An array of hydrogen-line profiles, from various locations in the Galaxy and the Magellanic Clouds.

35

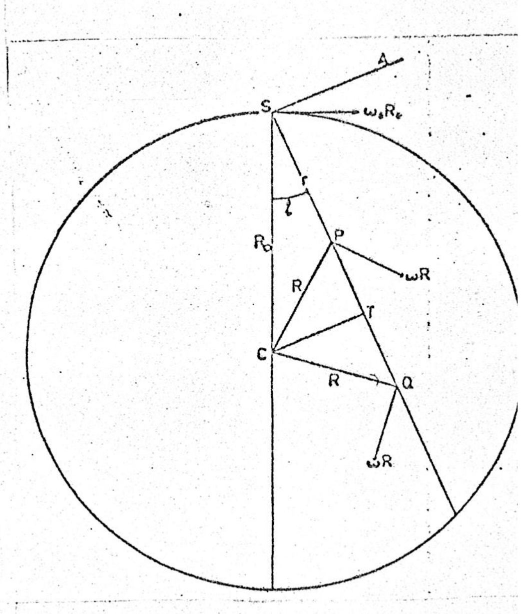

37

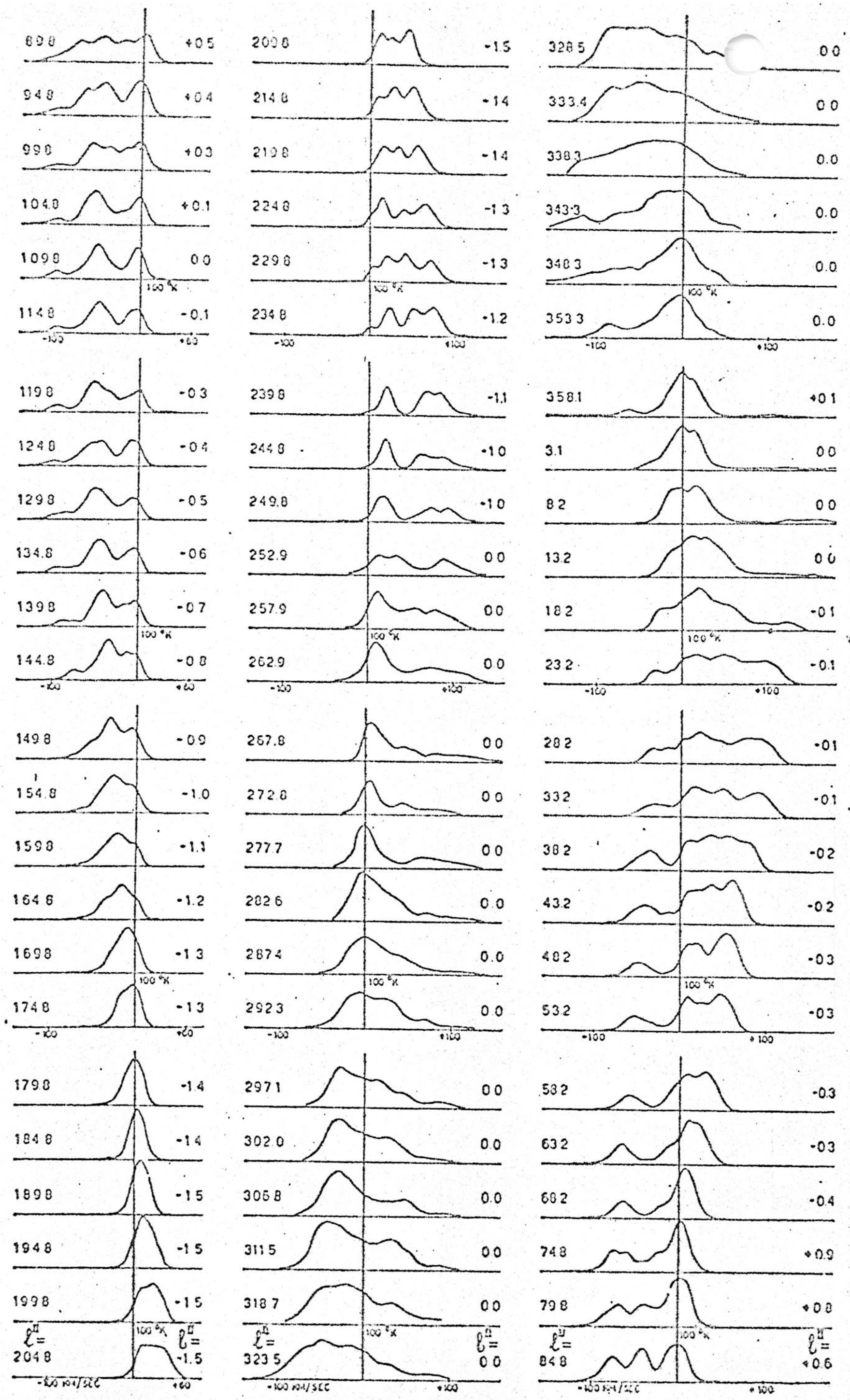

FIG. 6.—21-cm line profiles at approximately 5° intervals in galactic longitude, near the galactic plane. Antenna half-width 1°5 to 2°5, bandwidth 8 km/sec.

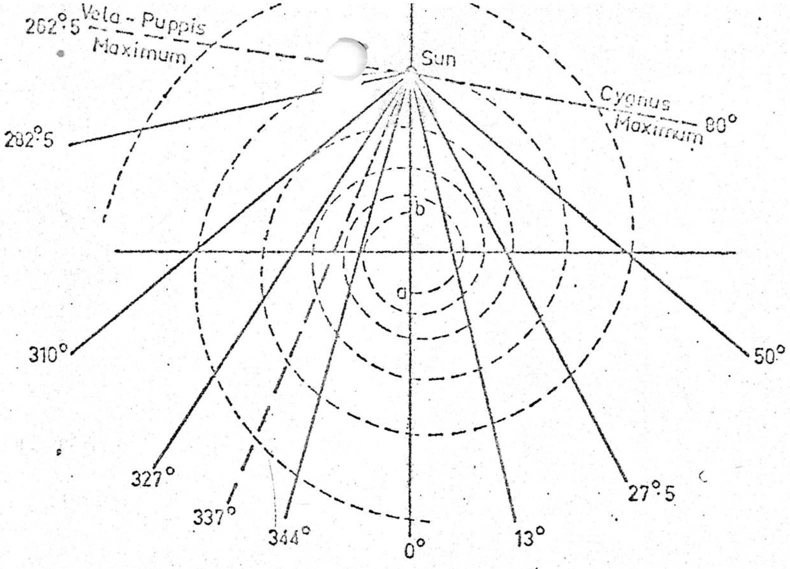

FIG. 7.—Direction of "steps" in the distribution of non-thermal radiation at 3.5 meter wavelength, and Mills' equiangular spiral fitting these steps (after Mills 1959*a*).

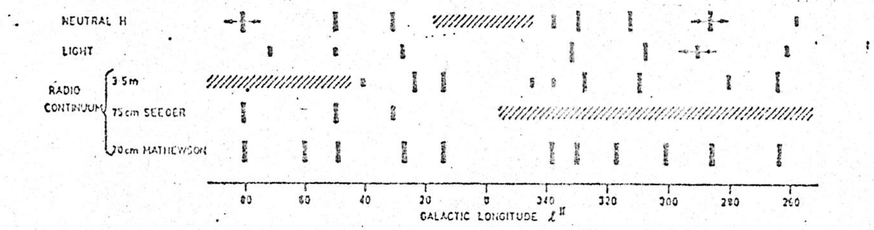

FIG. 8.—Tangential directions of spiral arms, for neutral hydrogen (Kerr 1962), light (Elsässer and Haug 1960), and radio-continuum radiation at 3.5 m. (Mills 1959*a*), 75 cm (Seeger *et al.* 1962), and 20 cm (Mathewson *et al.* 1962). *Shaded intervals:* not covered by observations

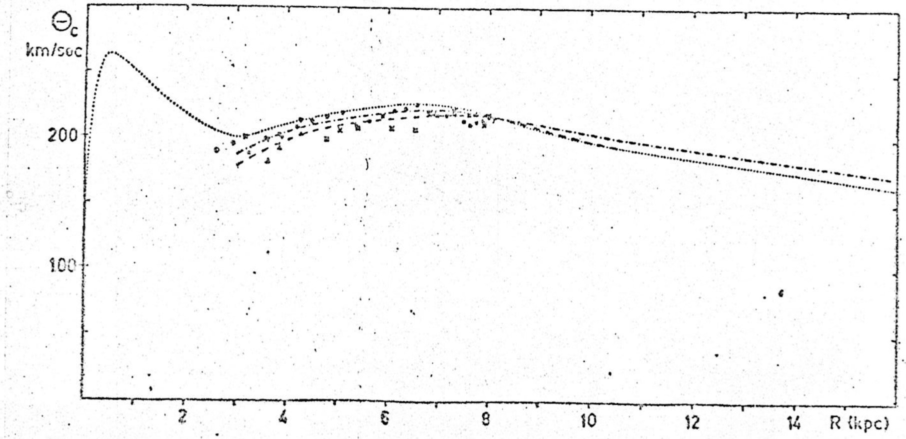

FIG. 3.—Possible rotation laws: ...... ($R < 8.2$ kpc) from northern hemisphere observations; ...... ($R > 8.2$ kpc) calculated from mass model (Schmidt 1956, model 2); ------ from southern hemisphere observations; -·-·- rotation velocity if solar neighborhood is moving out-

V (6

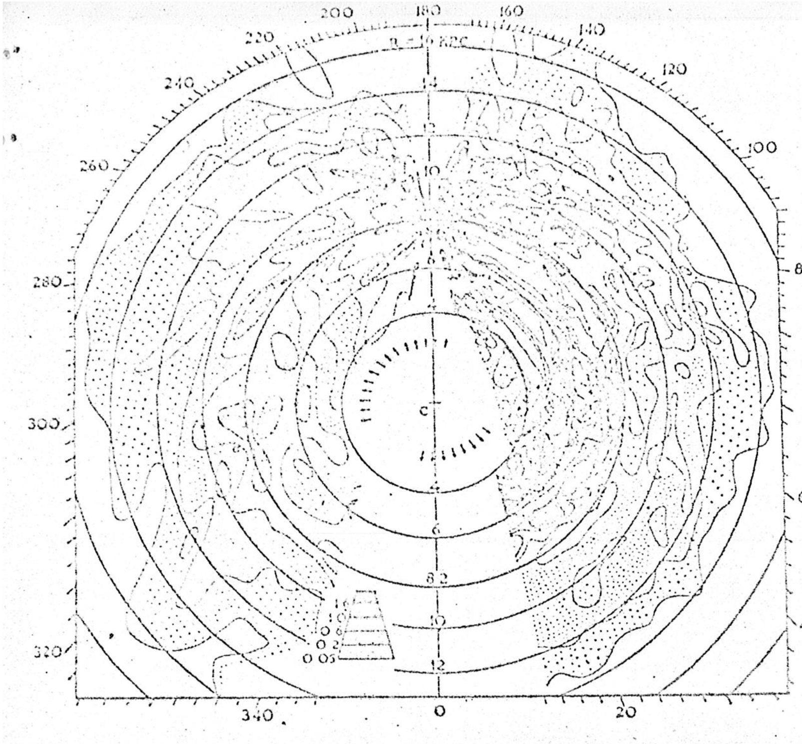

PLATE I.—Distribution of neutral hydrogen in the Galaxy (unit = atom/cm³) based on the …rthern hemisphere circular orbit model (Fig. 4, curve .... in Fig. 3).

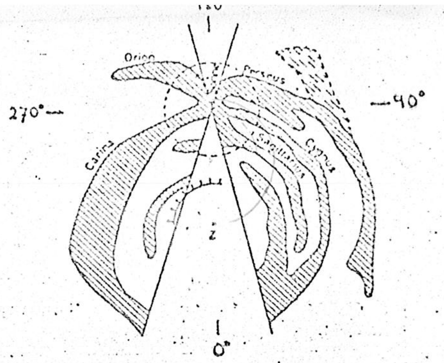

40 ↑

43 ↓

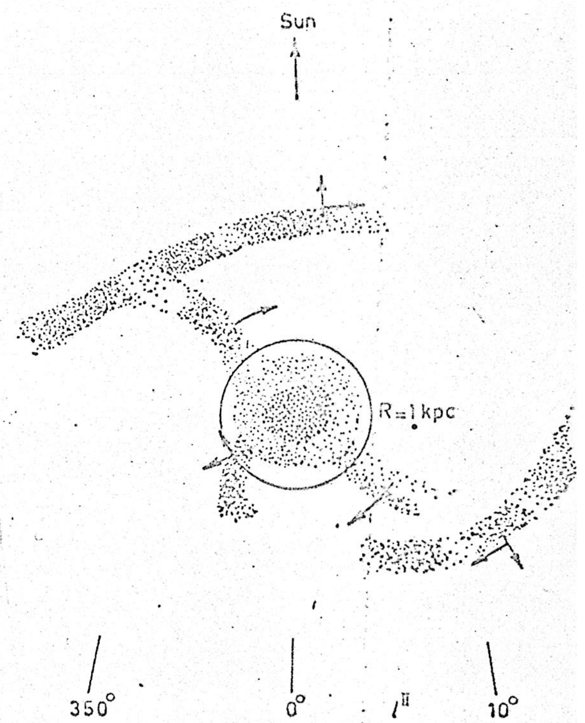

A possible structure for the galactic-centre reg…

← 41

42 ↓

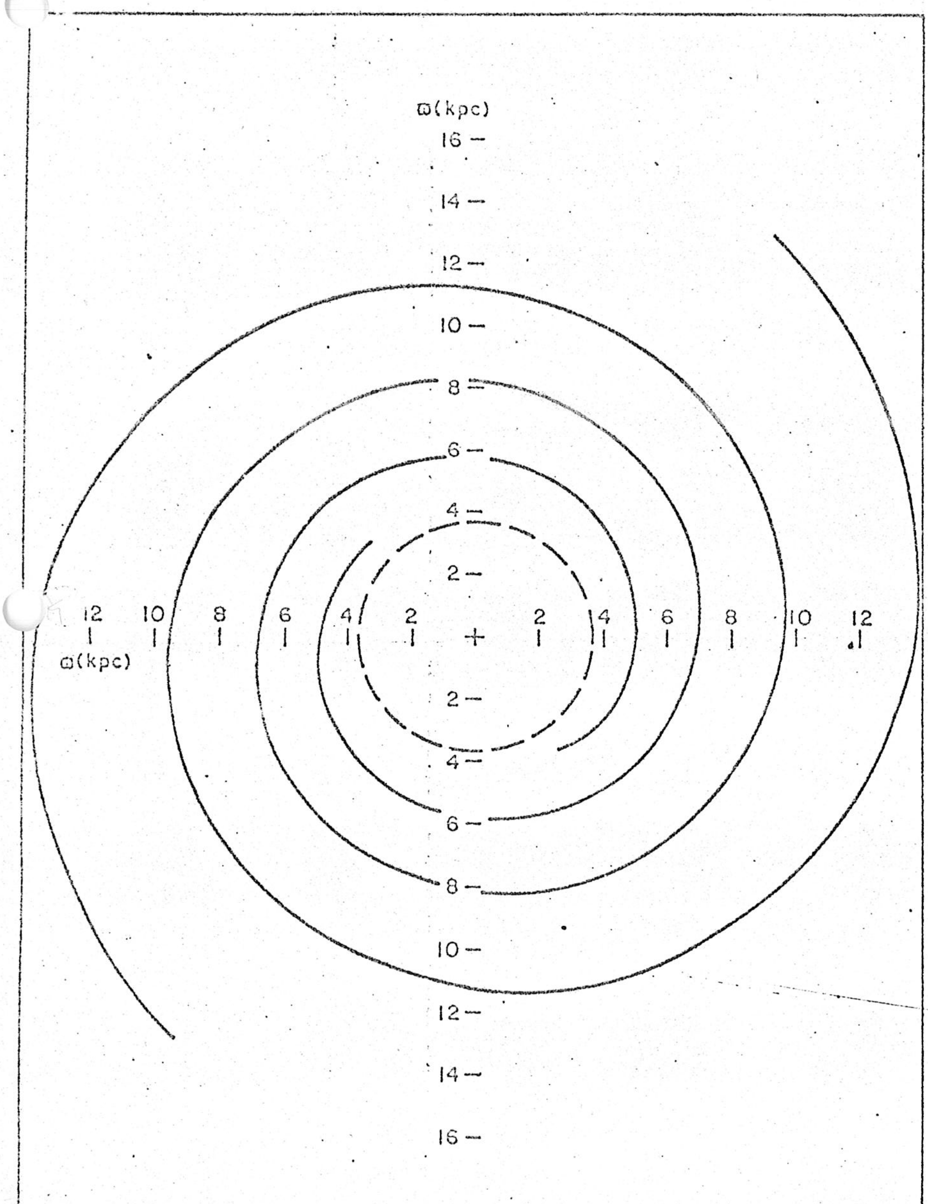

FIG. 3. Spiral pattern calculated for the 1965 Schmidt model, on the assumption that the pattern rotates at an angular velocity of 11 km sec⁻¹ kpc⁻¹ in the general direction of the rotation. Dispersion ring for Lindblad resonance taken at 3.75 kpc from the center.

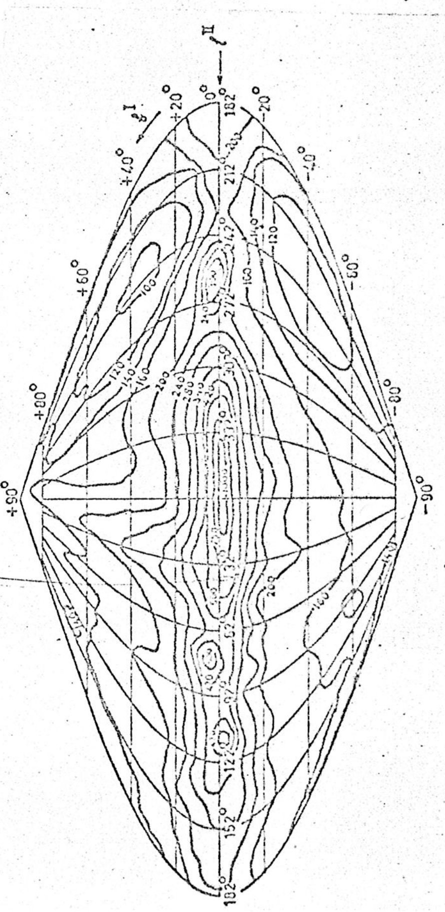

FIG. 1.—A low resolution (beam 17° × 17°) map showing the distribution of brightness temperature at 1.5 m over the whole sky (Dröge and Priester 1956). (Coordinates are old l^I and …

V (9)

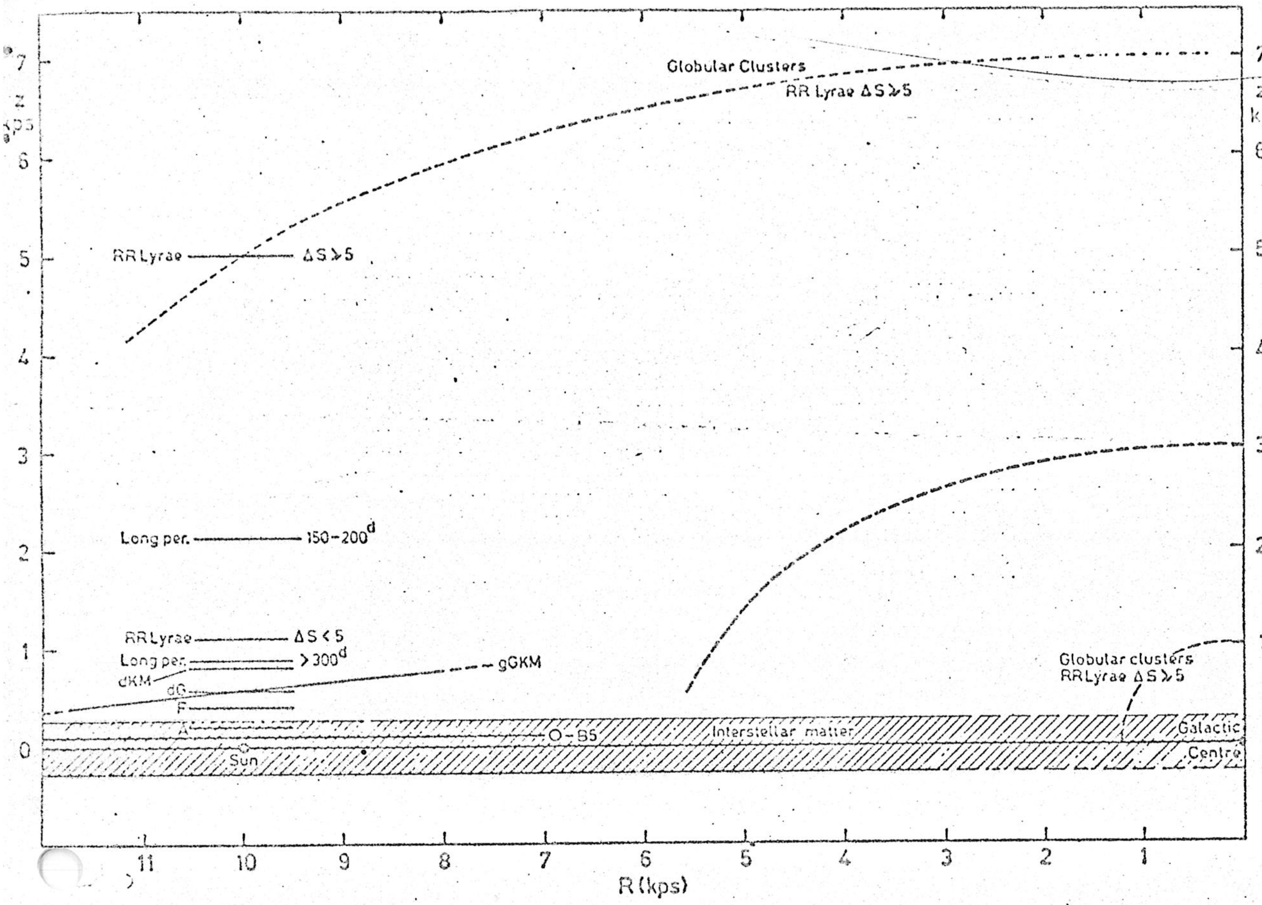

46 ↓

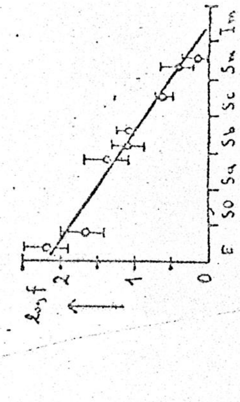

Fig. 1.—Schematic representation of the space distribution of the principal objects listed in Table 1, in a meridional cross-section of the Galaxy through the sun. The horizontal lines in the left-hand part indicate the levels z(0.1) given in column (2). The spheroidal distributions exhibited by the globular clusters and RR Lyrae variables are indicated by the elliptical contours.

44 ←

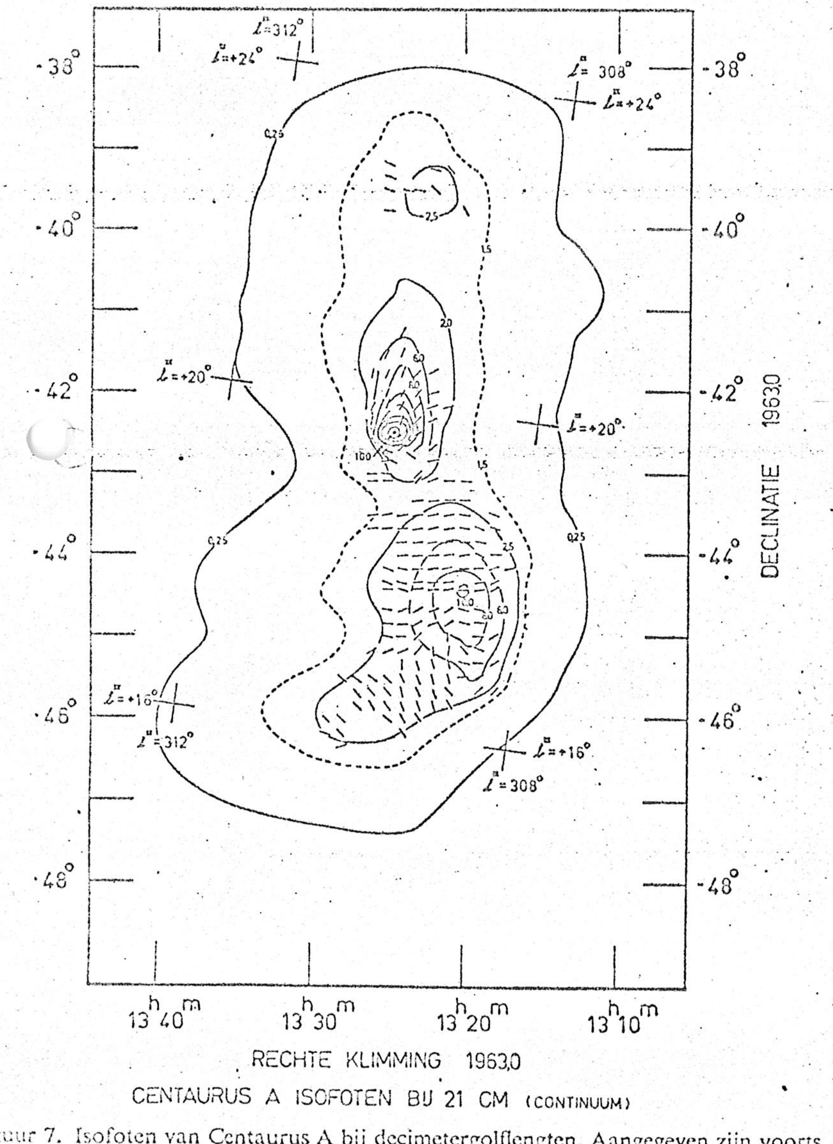

45 ↓

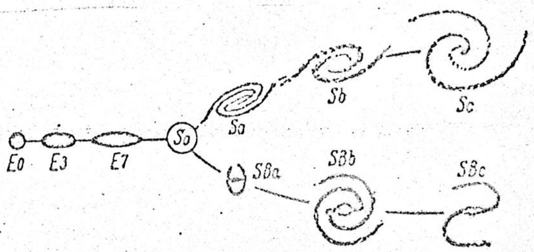

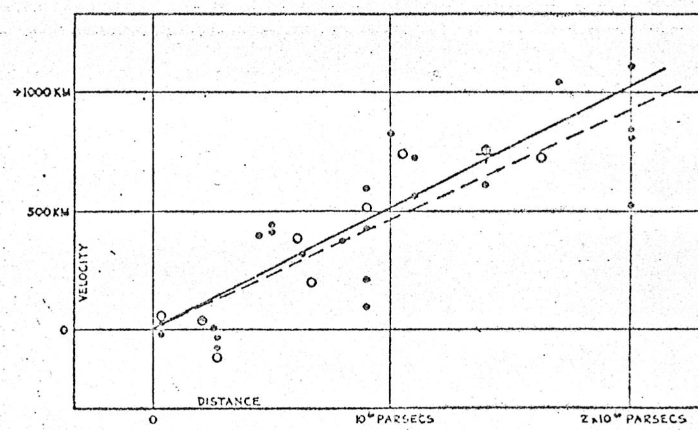

FIGURE 1

Velocity-Distance Relation among Extra-Galactic Nebulae.

Radial velocities, corrected for solar motion, are plotted against distances estimated from involved stars and mean luminosities of nebulae in a cluster. The black discs and full line represent the solution for solar motion using the nebulae individually; the circles and broken line represent the solution combining the nebulae into groups; the cross represents the mean velocity corresponding to the mean distance of 22 nebulae whose distances could not be estimated individually.

…guur 7. Isofoten van Centaurus A bij decimetergolflengten. Aangegeven zijn voorts richtingen van het gemiddelde magneetveld, zoals die volgen uit polarisatiewaar-

V (10)

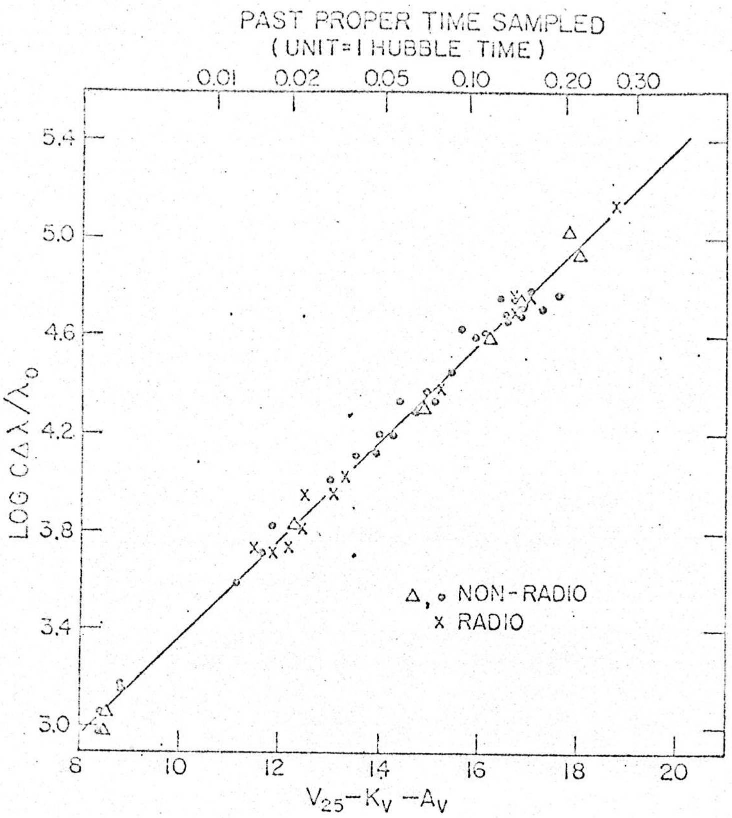

Fig[illegible]4. *The Hubble diagram of first-ranked cluster galaxies in 41 clusters. Dots are non-radio gala[illegible] crosses are radio galaxies, and open triangles are data by Baum for eight clusters, some of which are duplicated. All photometry is photo-electric and was obtained with the 200-inch Hale telescope. Correction for aperture effect, for K dimming, and for galactic absorption have been applied. The line has a slope of 5·0 and has been fitted to the data only in zero point.*

48b ↑

Fig. 50b

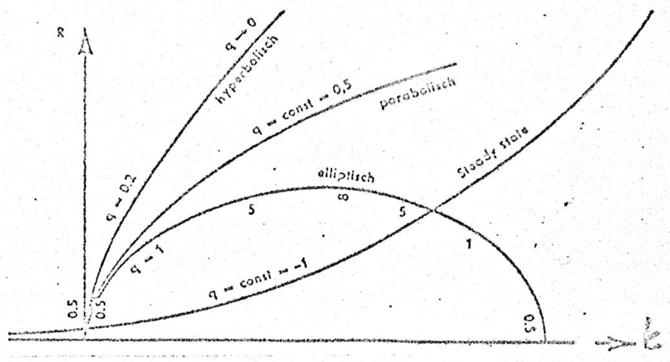

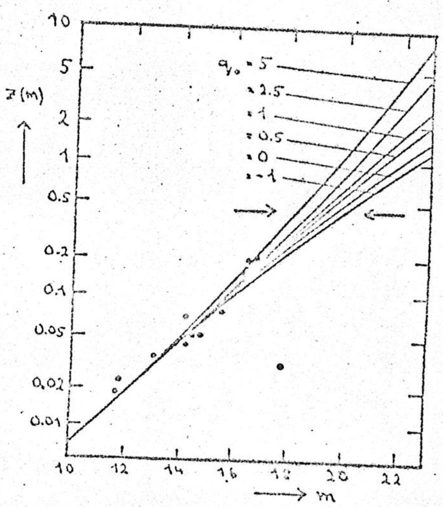

49 ↑

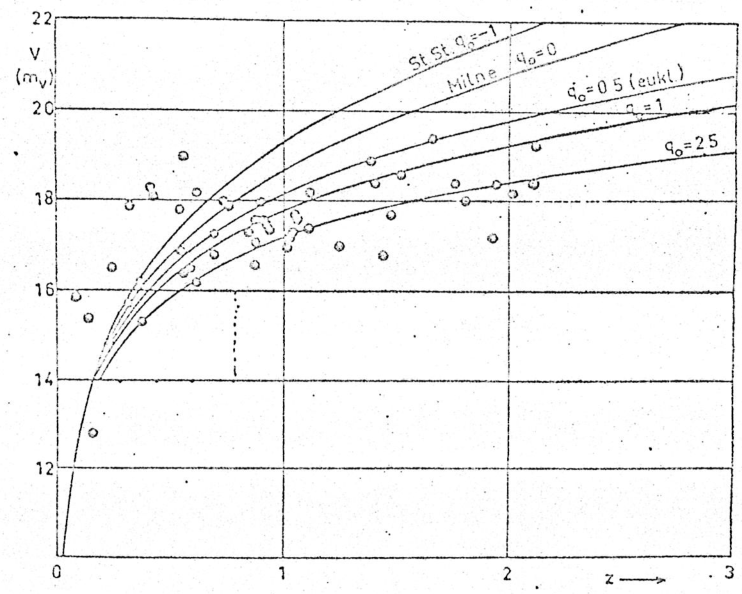

Fig. 8. Schijnbare helderheid van de QSO's is tegen de roodverschuiving uitgezet. De krommen geven het theoretisch verloop aan in de verschillende kosmologische modellen

St. st. = steady state

$0 < q_0 < 0,5$ is een hyperbolisch eeuwig uitdijend heelal

$q_0 > 0,5$ is een sferische heelal, dat op een later tijdstip weer inkrimpt

$q_0 = 0,5$ is een euklidisch heelal.

50a ←

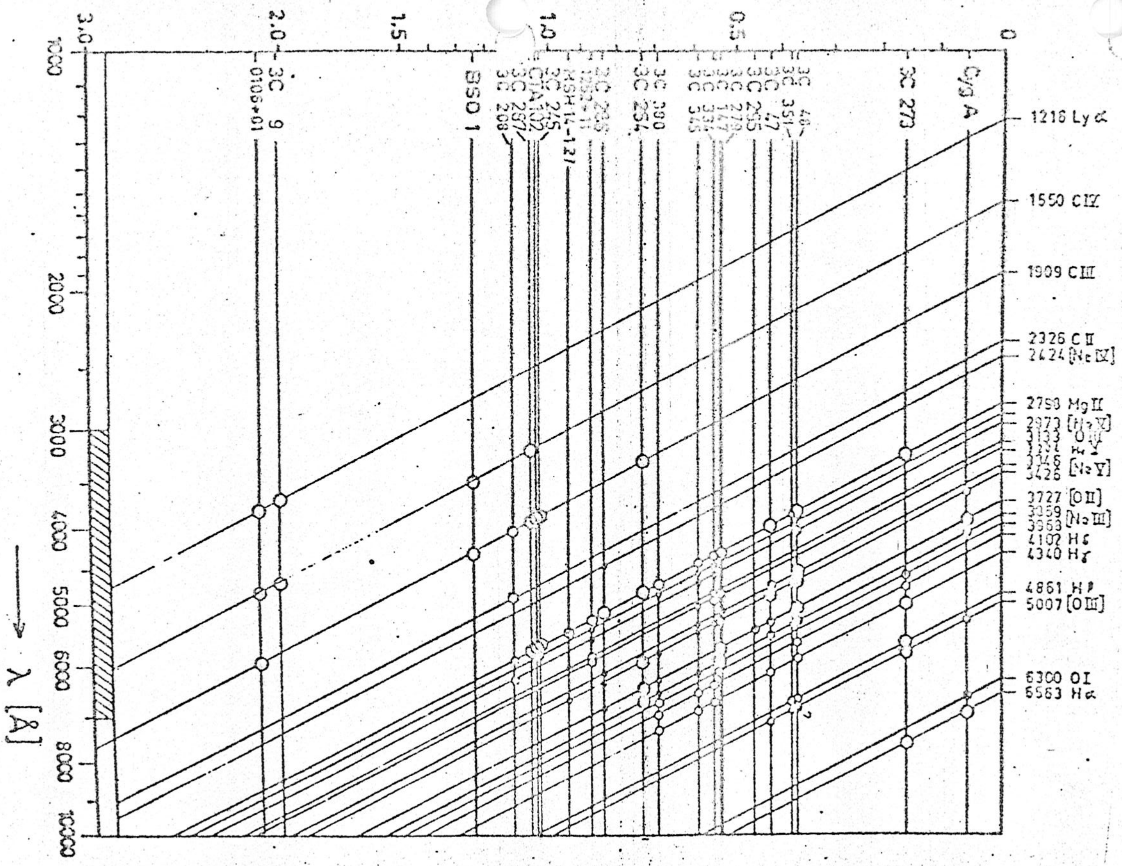

Fig. 5. Schematische emissielijn-spectra en roodverschuivingen van QSO's.
Grote cirkels: relatief sterke lijnen.
Kleine cirkels: relatief zwakke lijnen.
[ ] duidt verboden lijnen aan.
Het gearceerde gedeelte van het spectrum wordt niet door de atmosfeer geabsorbeerd en is dus waarneembaar.

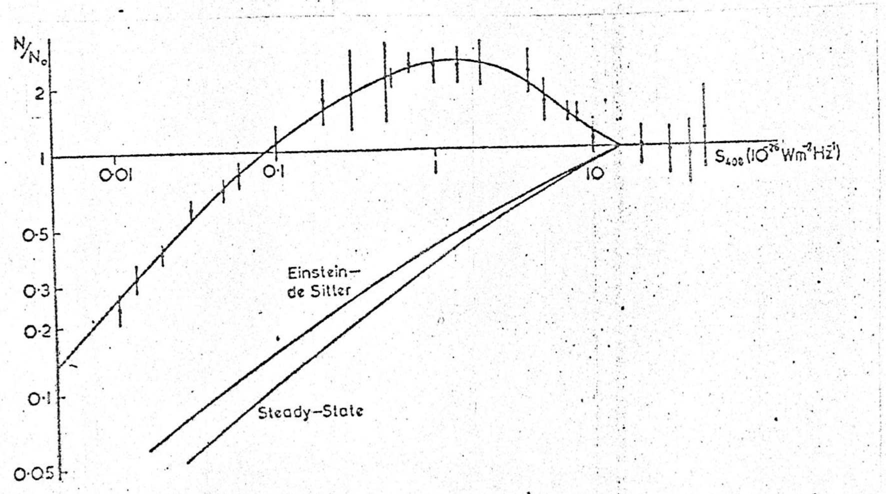

FIG. 3. The source counts presented as a curve of log (N/N_0) against log S, where N_0 is the number of sources per steradian which would be observed with a flux density greater than S in a static Euclidean universe. The corresponding curves for steady-state and source-conserving Einstein-de Sitter cosmologies are also shown.

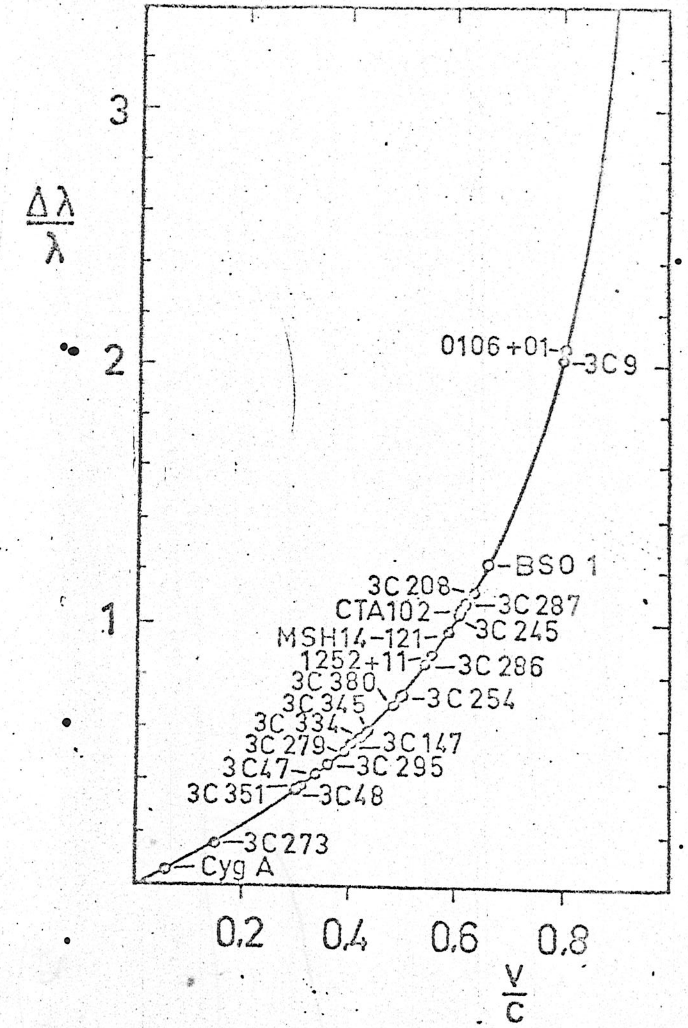

De snelheden van de QSO's als functie van hun roodverschuivingen worden gegeven door de formule:

$$1 + z = \left(1 + \frac{v}{c}\right)\left(1 - \frac{v^2}{c^2}\right)^{-\frac{1}{2}}$$

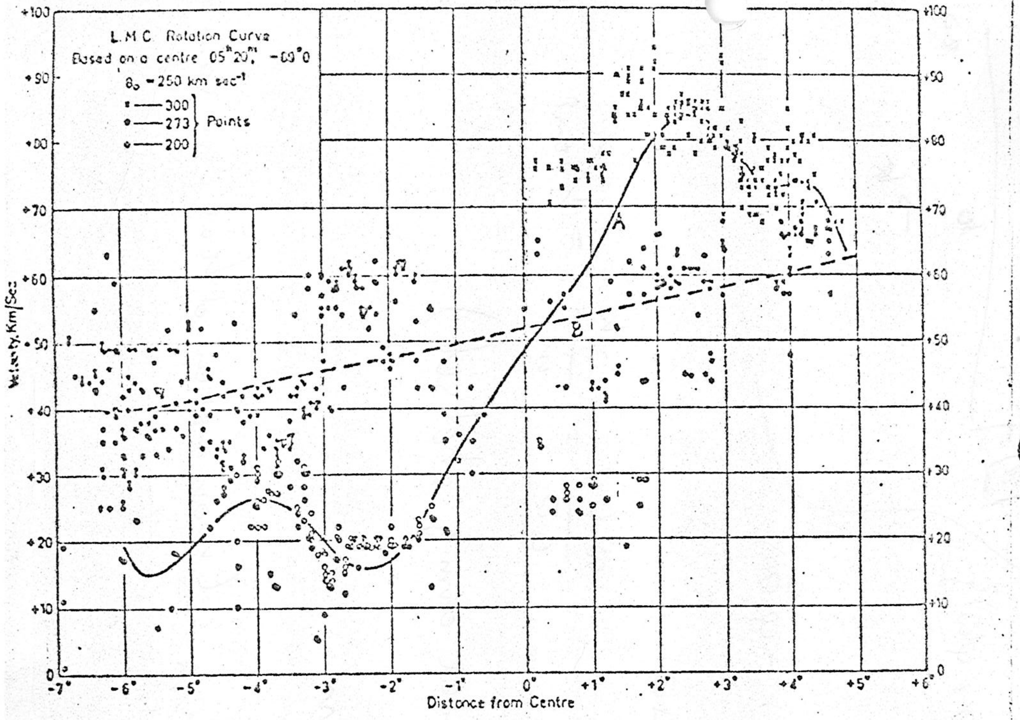

Fig. 13. LMC rotation curves on the model with two groups of spiral arms. Coordinates are radial velocity and distance from the 'center'. The points occur in a section ±10° from position angle 171°. Curve A has been fitted to the '+300' and '+243' points, and curve B to the '+273' points (McGee and Milton, 1966).

fig 54

Model Category	Acc. factor q_0	Density Param. σ_0	Cosmical constant ΛT_0^2	Space-Curv. Const. k	A (Age = AT_0)
A1(i)	0	0	0	−1	1·00
	0·5	0	−1·5	−1	0·87
A2(v)	1·0	0	−3·0	−1	0·79
	2·0	0	−6·0	−1	0·68
	0·02	0·02	0	−1	0·94
A1(ii)	0·15	0·15	0	−1	0·81
	0·2	0·2	0	−1	0·78
A1(iii)	0·5	0·5	0	0	0·67
	0·6	0·6	0	+1	0·64
A1(iv)	1·0	1·0	0	+1	0·57
	2·0	2·0	0	+1	0·47
	0·2	0·02	−0·54	−1	0·89
	0·5	0·02	−1·44	−1	0·84
	0·65	0·15	−1·5	−1	0·73
	1·02	0·02	−3·0	−1	0·76
A3	1·15	0·15	−3·0	−1	0·68
	2·02	0·02	−6·0	−1	0·66
	2·15	0·15	−6·0	−1	0·61
	1·0	0·8	−0·6	+1	0·59
	0·15	0·35	+0·6	−1	0·73
	0	0·33	+1·0	0	0·76
A2(vi-c)	−0·9	0	+2·7	−1	1·92
A2(vi-b)	−1·0	0	+3	0	∞

VI.1

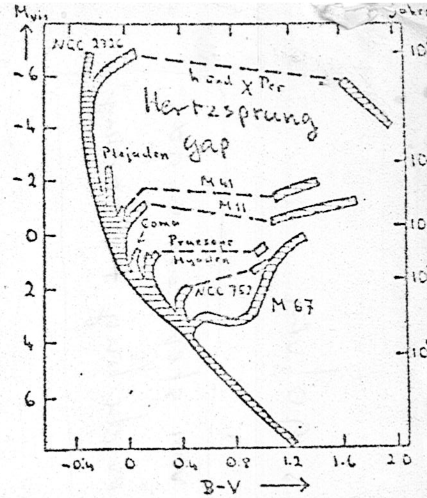

(Farbenhelligkeits-Diagramm)

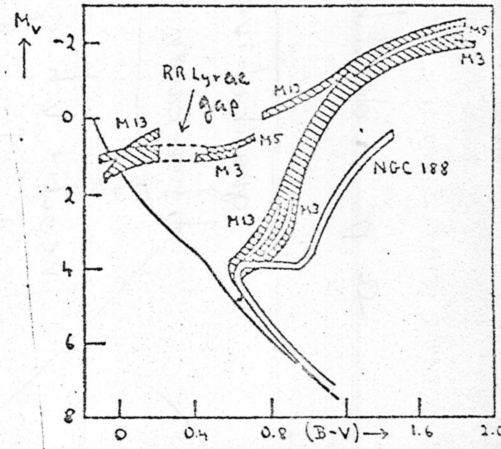

Zum Vergleich: NGC 188 = ältester bekannter offener Haufen. (Zwischenstellung)

VI.2

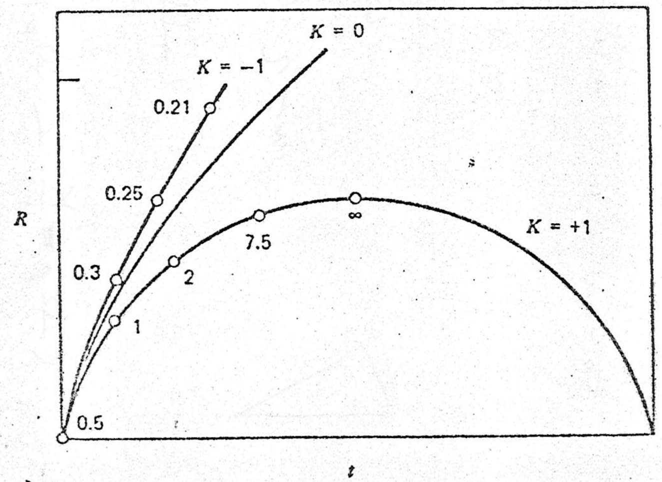

Figure 15.1 Solutions of Einstein's equations for a Robertson-Walker universe with curvature $k = +1$, $k = 0$, and $k = -1$. The numbers along the curves $k = \pm 1$ give the values of the deceleration parameter q_0 at various epochs.

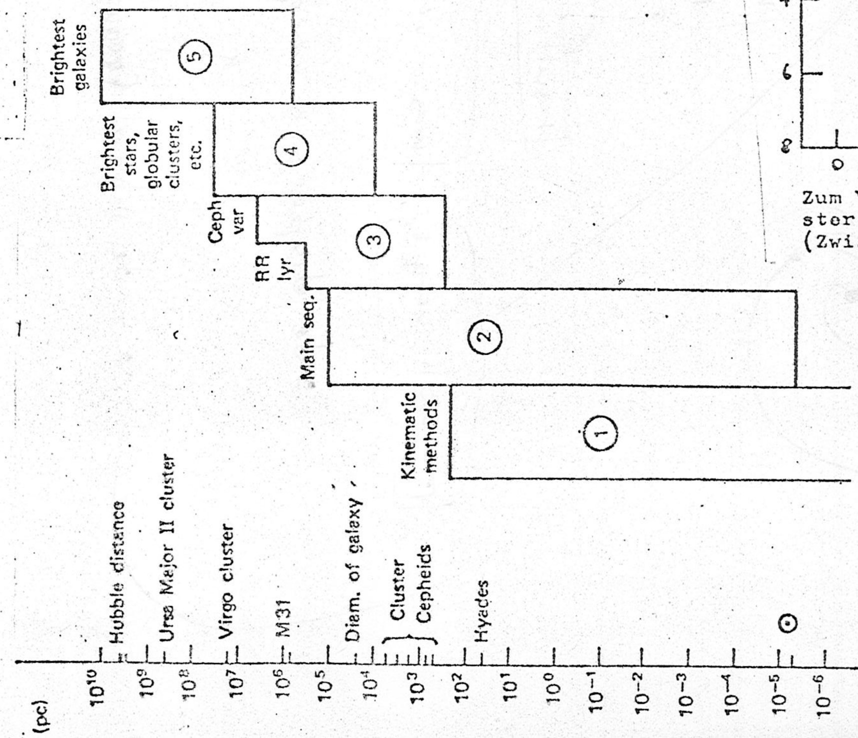

V.12